

# Absorbed Dose Assessment from Short-Lived Radionuclides of Radon ( $^{222}\text{Rn}$ ) Decay Chain in Lung Tissue: A Monte Carlo Study

Zohreh Danaei<sup>1</sup>, Hamid Reza Baghani<sup>1\*</sup>, Ali Asghar Mowlavi<sup>1</sup>

1. Physics Department, Hakim Sabzevari University, Shohad-e Hastei Blvd, Sabzevar, Iran

ARTICLE INFO	ABSTRACT
<b>Article type:</b> Original Article	<b>Introduction:</b> Internal exposure to radon gas progeny can lead to serious biologic damages to the lung tissue. The aim of this study was to evaluate the absorbed dose by lung tissue due to the exposure from short-lived radioactive products of radon ( $^{222}\text{Rn}$ ) decay using Monte Carlo simulation.
<b>Article history:</b> Received: Mar 09, 2019 Accepted: Des 22, 2019	<b>Material and Methods:</b> A lung equivalent phantom including 64 air sacs was simulated by MCNPX code. Then, the absorbed dose from short-lived radioactive products of radon decay chain including $^{218}\text{Po}$ , $^{214}\text{Po}$ , $^{214}\text{Pb}$ and $^{214}\text{Bi}$ was calculated for both suspended and deposited states of daughter nuclides inside the lung.
<b>Keywords:</b> Radon Radon Progeny Lung Dosimetry Monte Carlo method	<b>Results:</b> The results showed that alpha decay has more contribution to the lung absorbed dose in comparison with the beta and gamma decay. Furthermore, the received dose by the lung was higher when the radon progenies were deposited inside the lung so that the maximum received dose to lung was 100 times higher than that of calculated in suspended state. <b>Conclusion:</b> Short-lived daughter radionuclides of radon decay chain, especially alpha emitter products, can be considered as dangerous internal radiation sources. The biological effects of these daughter radionuclides is more severe when are suspended inside the respiratory system.

► Please cite this article as:

Danaei Z, Baghani HR, Mowlavi AA. Absorbed Dose Assessment from Short-Lived Radionuclides of Radon ( $^{222}\text{Rn}$ ) Decay Chain in Lung Tissue: A Monte Carlo Study. Iran J Med Phys 2020; 17: 66-74. 10.22038/ijmp.2019.38027.1486.

## Introduction

Radon (Rn) is a radioactive gas mainly derived from the decay chain of Uranium series [1]. The most important radioisotope of radon is  $^{222}\text{Rn}$ , which is one of the  $^{238}\text{U}$  progeny. The radon gas can be easily produced inside the soil and rocks [2], and gradually diffuse to the earth surface through the soil gas infiltration [3]. The concentration of emanated radon gas from the soil is different in the various seasons of the year. In fact, radon gas is more concentrated in fall and winter, compared to spring and summer due to the temperature inversion phenomenon occurring in cold seasons [4].

The soil gas infiltration, dissolved radon in the drinking water, and emanated radon from building materials [5] are the main sources of general exposure to radon gas. Based on the US Environmental Protection Agency (EPA) regulation, the radon level in drinking water should be less than 300 pCi/L [6]. Furthermore, according to the International Commission on Radiological Protection (ICRP) recommendation, the permissible level of radon gas in buildings is reported to range within 200-300 Bq/m<sup>3</sup> [7].

Internal exposure to radon gas can lead to dangerous biologic effects. According to US-EPA

estimations, internal exposure to radon gas causes about 15000 lung cancers per year [8]. Therefore, researchers have been motivated to widely evaluate radon gas concentration in different areas and its corresponding biological effects [9- 15].

Inhalation of radon gas is the most probable pathway for the entrance of this radioactive gas into the body. The penetration of this gas into the body can induce serious damages to the lung tissue through the production of short-lived alpha, beta, and gamma emitter daughter nuclides. The radioactive radon progeny can enter the lung through two different pathways. In the first case, the radon gas directly enters the respiratory system through breathing and releases daughters of radionuclides remaining inside the lung air sacs as the dust particles (suspended state). In the second one, the daughter radionuclides of the radon gas are produced outside the body and enter the lung after attaching to the ambient aerosols and deposit on the air sacs of the inner walls of lungs (deposited state).

Although several studies have been conducted to examine the mean concentration of this radioactive gas in different regions [13-19], less attention has been paid to the received dose by the lung due to its

\*Corresponding Author: Tel: +985144013216. E-mail: Hamidreza.baghani@gmail.com

short-lived progeny. Therefore, the aim of this study was to evaluate the received dose by the lung through the internal exposure to the short-lived daughter nuclides of <sup>222</sup>Rn decay chain in the two above mentioned states (suspended and deposited state) using Monte Carlo simulation.

### Materials and Methods

In order to evaluate the absorbed dose from the short-lived products of radon decay chain, a lung equivalent phantom was modeled using MCNPX 2.6.0 (LANL, USA) [20] Monte Carlo code. The geometry of the simulated lung phantom included 64 separate air sacs designed in 4 equal rows. The wall density of air sacs (soft tissue equivalent), located inside the lung phantom, was considered as 1.04 g/cm<sup>3</sup>. Moreover, the density of the air within the sacs was equal to 0.00125 g/cm<sup>3</sup>. The space between the simulated air sacs was considered as the lung tissue with the density of 0.296 g/cm<sup>3</sup>. The total length of simulated lung phantom in each side was equal to 0.086 cm. Regarding the fact that air sacs account for about 87% of lung volume [21, 22], the radius of each spherical air sac inside the lung phantom was estimated as 0.0127 cm. A three-dimensional view from simulated lung phantom along with the considered air sacs is shown in Figure 1.

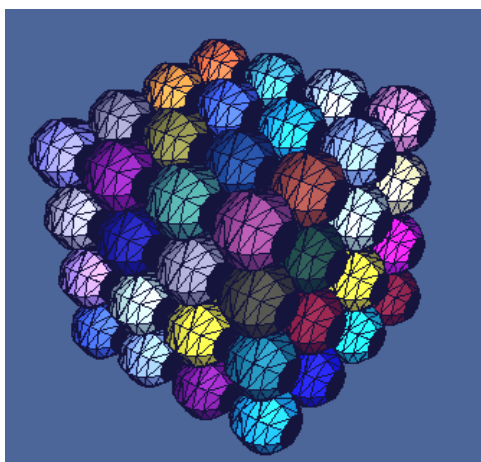
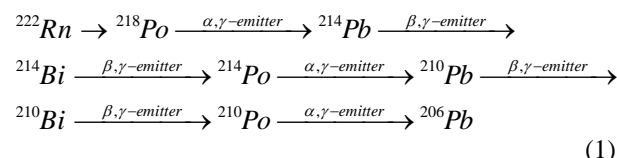


Figure 1. A three-dimensional view from simulated lung phantom consisting of 64 separate air sacs within the phantom

Short-lived radon progenies in the present study included <sup>218</sup>Po, <sup>214</sup>Po, <sup>214</sup>Pb, and <sup>214</sup>Bi [23, 24]. As previously mentioned, these radioactive products were evaluated in two different physical states. At the first state, the daughter products were considered as the suspended particles inside the air sacs [25]. In the second scenario, the radioactive products were assumed as the deposited particles on the inner surface of the simulated air sacs [26]. The main difference between these two simulated states referred to the position and geometry of the radiation source. The radiation source in the first case was a solid spherical one, which completely filled the inner volume of all simulated air sacs within the lung phantom. On the other hand, a

spherical shell with 1 μm thickness was considered as the radiation source in the second case, which was located on the inner surface of each simulated air sac within the lung phantom. In both cases, a uniform spatial distribution was used for the simulated radiation sources.

The decay chain of <sup>222</sup>Rn and the decay mode of each progeny is presented in the scheme bellow [27]:



All physical characteristics of the investigated progenies, including alpha, beta, and gamma energy spectrum, as well as the corresponding half-life were taken from Radionuclide Data and Decay Schemes (MIRD) [28]. The summary of the physical characteristics of the investigated radon progenies are reported in tables 1-3. Due to the very long half-life of <sup>210</sup>Pb (22.3 years), this radioisotope and its subsequent decay products were not considered in the performed simulations.

Table 1. Alpha-emitter progeny of radon decay chain and corresponding physical characteristics

Daughter nuclide	Emitted energy per transition (MeV/decay)	Half-life
<sup>218</sup> Po	6.113	3.10 min
<sup>214</sup> Po	7.833	164.3 μsec

Table 2. Beta-emitter progeny of radon decay chain and corresponding physical characteristics

Daughter nuclide	Mean emitted energy per decay (MeV/decay)	Half-life
<sup>214</sup> Pb	0.295	26.8 min
<sup>214</sup> Bi	0.663	19.9 min

Table 3. Gamma-emitter progeny of radon decay chain and corresponding physical characteristics

Daughter nuclide	Mean emitted energy per transition (MeV/decay)	Half-life
<sup>214</sup> Bi	1.479	19.9 min
<sup>214</sup> Po	0.253	164.3 μsec

Regarding the serial production of these radioactive daughter nuclides in the radon decay chain, a weighting factor was considered for each daughter nuclide. As mentioned earlier, two different physical states were investigated in the current study. In the case that the radon progenies were deposited on the simulated air sacs, there would be no chance for the escape of daughter radionuclides from the lung.

$$\begin{aligned}
 W_{218Po} &= \text{Decay probability at one breathing cycle} = 1 - e^{-\lambda_{218Po}t} \\
 W_{214Pb} &= \text{Decay probability at one breathing cycle} = (1 - e^{-\lambda_{218Po}t})(1 - e^{-\lambda_{214Pb}t}) \\
 W_{214Bi} &= \text{Decay probability at one breathing cycle} = (1 - e^{-\lambda_{218Po}t})(1 - e^{-\lambda_{214Pb}t})(1 - e^{-\lambda_{214Bi}t}) \\
 W_{214Po} &= \text{Decay probability at one breathing cycle} = (1 - e^{-\lambda_{218Po}t})(1 - e^{-\lambda_{214Pb}t})(1 - e^{-\lambda_{214Bi}t})(1 - e^{-\lambda_{214Po}t})
 \end{aligned} \tag{2}$$

$t = 3 \text{ sec}$   
 $\lambda = \text{decay constant}$

Therefore, all of these daughter nuclides would deposit their emitted energies inside the lung. As a result, the weighting factor of all studied progenies were equal to one at the deposited state. On the other hand, when the daughter nuclides were considered as the suspended particles inside the air sacs, there would be always a finite probability for the escape of each radon progeny from the respiratory system. Therefore, a specific weighting factor should be considered for each daughter nuclide based on its half-life and priority in the radon decay chain. Considering the mean time duration of 3 seconds for each normal respiratory rate (including inspiration and expiration) [29], these weighting factors can be calculated according to the equation below (based on the general radioactive decay law):

The calculated weighting factors for radon progeny are reported in Table 4.

Table 4. Weighting factors related to different progeny of radon in a single decay chain of radon gas

Daughter nuclide	Weighting factor (w) in a decay chain
<sup>218</sup> Po	0.011
<sup>214</sup> Pb	1.44E-5
<sup>214</sup> Bi	2.5E-8
<sup>214</sup> Po	2.5E-8

In order to evaluate the received dose to the different parts of the lung tissue, the dose profiles which pass through the center of simulated air sacs were calculated inside the modeled lung phantom. Dose calculations were performed using the \*F8 scoring tally (the gold standard scoring tally for radiation dosimetry by MCNP code).

It should be mentioned that 10<sup>9</sup> histories were transported in each simulation and the associated statistical error to the obtained results was less than 3% in all the performed simulations.

## Results

The dose profiles related to the two short-lived alpha emitter daughter nuclides of <sup>218</sup>Po and <sup>214</sup>Po in suspended and deposited physical states inside the lung are shown in figures 2 and 3, respectively. It should be

mentioned that all of the presented results are corresponding to a single radon decay chain.

As can be seen in Figure 2, the contribution of <sup>218</sup>Po daughter nuclide to the received dose by lung tissue is several orders of magnitude (10<sup>5</sup>) higher than the <sup>214</sup>Po. The maximum lung dose due to the exposure to <sup>218</sup>Po and <sup>214</sup>Po was about 79 nGy and 0.18 pGy, respectively. On the other hand, as shown in Figure 3, the <sup>218</sup>Po and <sup>214</sup>Po have almost the same contribution in the received dose by the lung tissue. Therefore, the maximum dose from both mentioned alpha emitter daughter nuclides in the deposited state was about 7 μGy.

The comparison of the results in figures 2 and 3 demonstrated that the overall dose received by the lung tissue, due to the exposure from alpha emitter progeny, was significantly higher in the deposited physical state, such that the maximum overall doses of alpha particles in deposited and suspended states were equal to 14 μGy and 79 nGy, respectively.

The dose profiles related to the beta emitter products of radon decay chain, including <sup>214</sup>Pb and <sup>214</sup>Bi, in the suspended and deposited physical states are shown in figures 4 and 5, respectively. The obtained results are corresponding to a single radon decay chain.

As indicated in Figure 4, the beta dose inside the lung was mainly due to the internal exposure to <sup>214</sup>Pb and <sup>214</sup>Bi, which had no significant contribution to the lung dose at the suspended state. The maximum doses related to the <sup>214</sup>Pb and <sup>214</sup>Bi inside the lung at the suspended state were equal to 0.42 pGy and 5.5×10<sup>-16</sup> Gy, respectively. On the other hand, the beta dose from <sup>214</sup>Bi was higher than that of <sup>214</sup>Pb at the deposited state (as indicated in Figure 5). The maximum beta doses for <sup>214</sup>Bi and <sup>214</sup>Pb at the deposited state were 30 nGy and 23 nGy, respectively.

The comparison of the calculated dose for beta particles indicated that the deposited daughter nuclides would result a more radiation dose inside the lung, compared the suspended ones. The maximum beta doses from beta emitter radionuclides of radon decay inside the lung were estimated as 53 nGy and 0.42 pGy for deposited and suspended states, respectively.

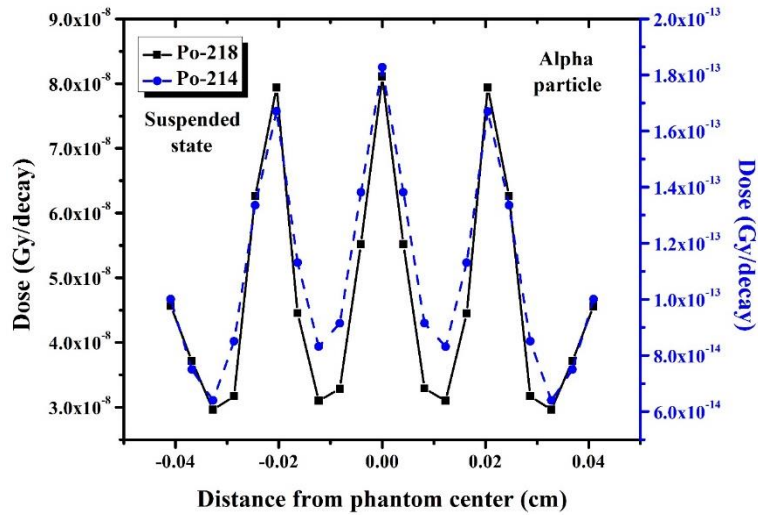


Figure 2. Dose profiles related to the short-lived alpha emitter products of each radon decay chain in suspended state inside the lung.

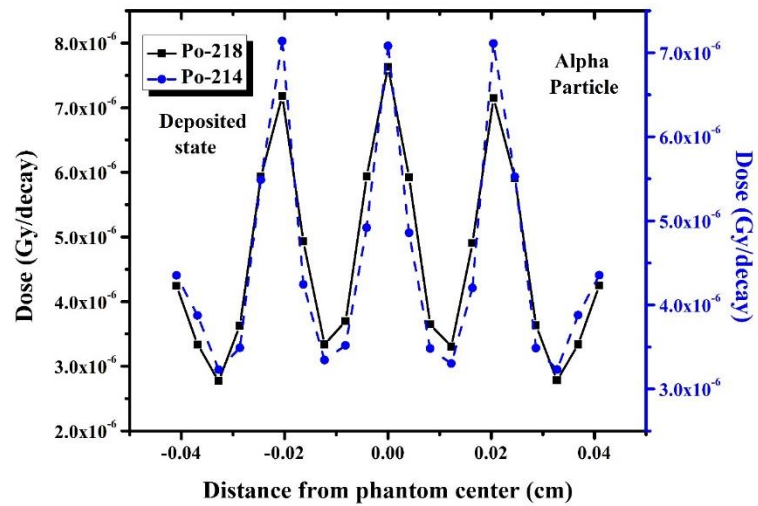


Figure 3. Dose profiles related to the short-lived alpha emitter products of each radon decay chain in deposited state inside the lung.

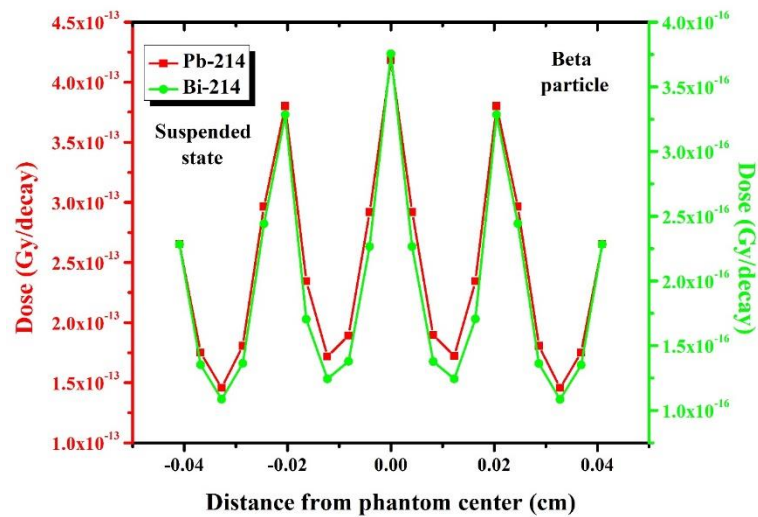


Figure 4. Dose profiles related to the beta emitter progeny of radon decay chain at the suspended state inside the lung.

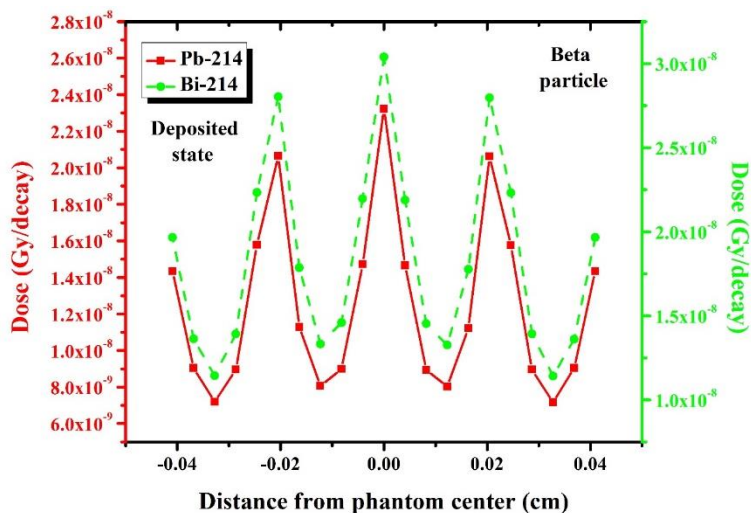


Figure 5. Dose profiles related to the beta emitter progeny of radon decay chain at the deposited state inside the lung.

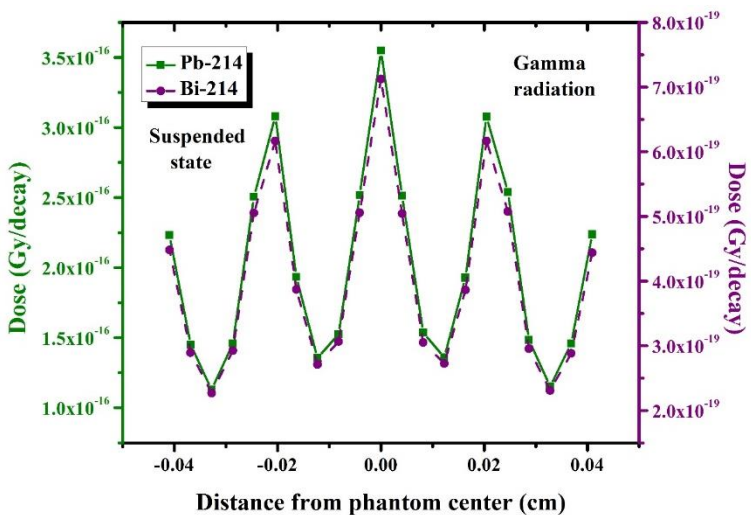


Figure 6. Dose profiles related to the short-lived gamma emitter products of each radon decay chain in suspended state inside the lung.

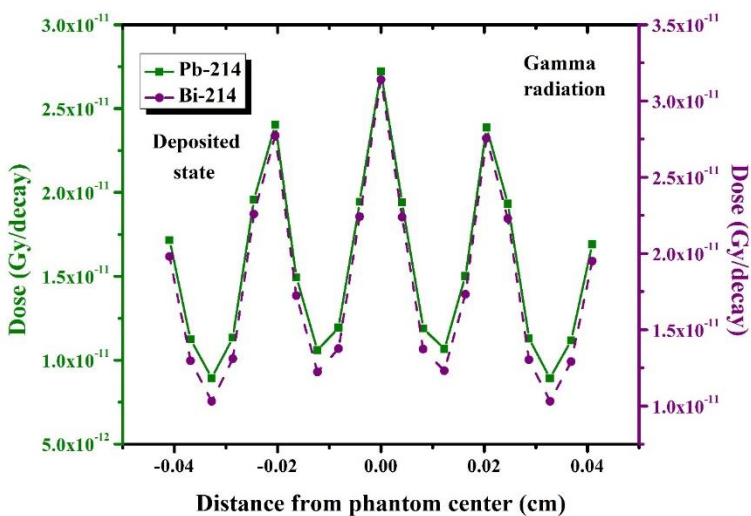


Figure 7. Dose profiles related to the short-lived gamma emitter products of each radon decay chain in deposited state inside the lung.

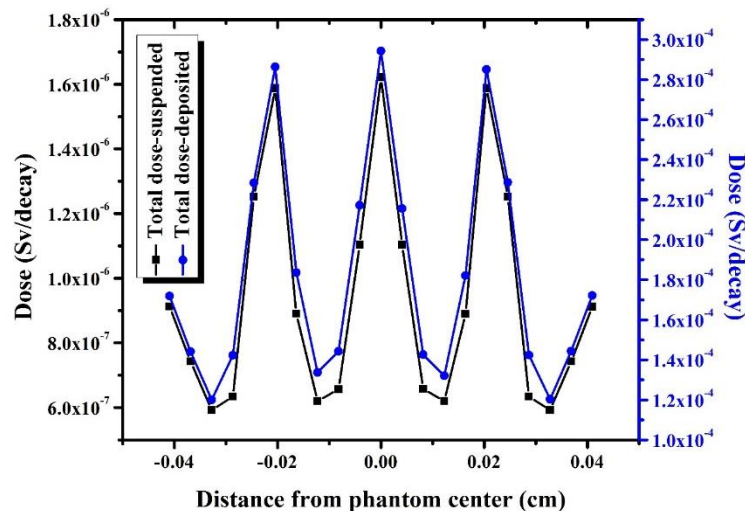


Figure 8. Comparison of the overall dose profiles related to the contribution of all short-lived progenies of radon in both suspended and deposited state inside the lung.

The dose profiles related to the gamma radiations of  $^{214}\text{Pb}$  and  $^{214}\text{Bi}$  at the suspended and deposited physical states are shown in figures 6 and 7, respectively. The reported dosimetry results in these figures are obtained for a single radon decay chain.

As illustrated in Figure 6, the gamma radiation emitted from  $^{214}\text{Pb}$  has the most association in the received dose by the lung and emitted gamma rays from  $^{214}\text{Bi}$  have a little contribution to the lung absorbed dose at the suspended state. The maximum received doses by the lung from gamma radiation of  $^{214}\text{Pb}$  and  $^{214}\text{Bi}$  at the suspended state was equal to  $3.5 \times 10^{-16}$  and  $7.1 \times 10^{-19}$  Gy, respectively. On the other hand, the emitted gamma radiation from  $^{214}\text{Bi}$  was more effective in the absorbed dose by the lung at the deposited state (Figure 7). The maximum lung doses related to the gamma rays emitted from  $^{214}\text{Pb}$  and  $^{214}\text{Bi}$  were equal to 27 pGy and 31 pGy, respectively.

The comparison between the dose profiles related to the contribution of all short-lived daughter nuclides at the suspended and deposited physical states inside the lung is shown in Figure 8. It should be mentioned that the radiation weighting factor of alpha, beta, and gamma radiation ( $w_R$ ) for equivalent dose calculations were taken from ICRP-103 [30]. As mentioned in this report,  $w_R$  for alpha particles is equal to 20, while this factor is considered as unity for beta and gamma radiation.

As depicted in Figure 8, the lung overall received dose from alpha, beta, and gamma emitter progeny of radon decay at the deposited state was higher than that of the suspended state. The maximum overall doses in suspended and deposited states were about 1.6  $\mu\text{Sv}$  and 290  $\mu\text{Sv}$  for each decay chain of radon gas, respectively.

## Discussion

The dose profiles related to the alpha, beta, and gamma radiations of radon decay products are demonstrated in figures 2-7. It should be mentioned that

two separate physical states, including suspended and deposited ones, were considered for the spatial distribution of radon progeny inside the lung and dose profile calculations were performed for each state.

The obtained dose profiles for alpha particles (refer to figures 2 and 3), showed that the  $^{218}\text{Po}$  has the maximum contribution to received dose by the lung tissue in the suspended state. This fact is due to the priority of this daughter nuclide in the radon decay chain and its short half-life which lead to the highest weighting factor for this radionuclide in the radon decay chain (refer to Table 4). With regard to the potential biologic hazard,  $^{218}\text{Po}$  is the most dangerous alpha emitter product of radon when it is suspended inside the lung's air sacs. On the other hand, both alpha emitter radionuclides had almost the same contribution in the lung dose at the deposited state inside the lung's air sacs. This issue can be justified by the equal weighing factor of  $^{218}\text{Po}$  and  $^{214}\text{Po}$  in radon decay chain at the deposited physical states and also analogues emitted alpha energy from these daughter radionuclides.

The calculated dose profiles for beta and gamma emitter products of radon decay, including  $^{214}\text{Pb}$  and  $^{214}\text{Bi}$ , showed that the absorbed dose by the lung through internal exposure from these radionuclides was higher in the deposited physical state. This finding can be attributed to the higher weighting factor of beta emitter progeny in the radon decay chain at the deposited state (refer to Table 4). For the suspended state,  $^{214}\text{Pb}$  had higher contribution to beta and gamma doses inside the lung due to the priority of this radionuclide in the radon decay chain and its higher weighting factor, compared to  $^{214}\text{Bi}$ . On the other hand,  $^{214}\text{Bi}$  would result to higher beta and gamma doses inside the lung at the deposited state, compared to  $^{214}\text{Pb}$ . Regarding the fact that all radon progenies have the same weighting factor in the radon decay chain at the deposited state and no priority was considered for radon decay products, higher beta and gamma energies of  $^{214}\text{Bi}$  respect to the  $^{214}\text{Pb}$  (refer

to tables 2 and 3) could contribute to such result at the deposited state.

As it can be seen in figures 2-7, the absorbed dose for each investigated particle would receive its maximum value at the phantom center (the interface between the adjacent air sacs where the wall of each air sac is located) and decrements in the areas adjacent to the center of each simulated spherical air sac. This finding could be expected at the deposited physical state since the radiation source was a spherical shell (with 1  $\mu\text{m}$  thickness) adjacent to the air sac walls. Therefore, it can be concluded that the received dose by the walls of each air sac would be higher than the absorbed dose at the center of each spherical air sac. The same trend was also observed at the suspended state, and the received dose by the wall of each air sac would be higher than that of air sac center at the suspended physical state. The underlying reasons for this issue could be firstly the uniform spatial distribution of radon progeny inside the spherical volume of each air sac, and secondly the higher density of air sac's walls, compared to the space within each air sac (soft tissue versus air with the densities of 1.04  $\text{g}/\text{cm}^3$  and 0.00125  $\text{g}/\text{cm}^3$ , respectively). Due to the higher density of air sac wall in comparison with the air within each air sac and also uniform irradiation of two mentioned media, it can be expected that the received dose by the air sac wall would be higher than that of the enclosed air-filled spherical volume of each air sac.

The comparison of the different lung dose components, including alpha, beta, and gamma dose showed that the alpha emitter products of the radon decay are the main contributors to the received dose by lung through the internal exposure to the radon progeny. Therefore, the alpha emitter daughter nuclides should be considered as the most dangerous products of radon decay, which can have a considerable biologic effect on the human respiratory system. This finding was in accordance with those recommended by Anjos et al [16]. In this study, the received dose by occupants of San Luis province (Argentina), due to the both radon gas and natural gamma radiation, was measured through  $\text{CaF}_2$  and LiF-100 TL dosimeters. Obtained results showed that the annual effective dose from gamma exposure is equal to 0.48  $\text{mSv}/\text{year}$ , while this value can reach to 28  $\text{mSv}/\text{year}$  in the case of radon gas inhalation.

The received dose by the lung through the internal exposure to radon and its progeny are reported in some studies. As presented by Kendall and Smith [31], the received dose by the lung from  $^{218}\text{Po}$ ,  $^{214}\text{Po}$ ,  $^{214}\text{Pb}$  and  $^{214}\text{Bi}$ , during the inhalation of the 1 Bq activity of the radon gas, is equal to  $6.6 \times 10^{-8}$ ,  $4.6 \times 10^{-14}$ ,  $3.6 \times 10^{-7}$ , and  $2.9 \times 10^{-7}$  Sv, respectively. The observed differences between our results and those reported by the mentioned study can be attributed to the different followed approaches for the dosimetry of the radon gas and its progeny inside the lung as well as the supposed geometry for the spatial distribution of the radiation source inside the lung. The obtained results of Kendall and Smith were based on the mathematical modeling of

internal radiation emitters inside the lung according to the ICRP-66 human respiratory track model [32]. However, the present study was performed based on the Monte Carlo modeling of the lung tissue along with its air sacs and direct transportation of different radiations inside the lung. Furthermore, the dose from different radiation emitters (including alpha, beta and gamma emitter daughter nuclides) have been investigated separately. On the other hand, an overall equivalent dose for each radionuclide were presented using Kendall and Smith without the consideration of the dose component for each type of emitted radiation in the radon decay chain.

Mostafa et al. also estimated the maximum received dose to the lung by the radon and its progeny by means of the human respiratory track model using ICRP-66 [18]. The results of this study showed that the maximum lung dose through the internal exposure to the radon and its daughter nuclides can reach 0.22  $\text{mSv}$  per year.

Yu et al. also calculated the effective dose of the lung through the internal exposure to radon decay chain [33]. This study was also based on employing the ICRP-66 human respiratory track model. The results of this research demonstrated that a dose conversion coefficient of 15  $\text{mSv}/\text{WLM}$  (working level month) should be considered for radon dosimetry inside the lung tissue.

Altshuler et al. also estimated the received dose through the respiratory system following the inhalation of the radon gas through nose breathing and exposure to its progeny [34]. The results of this study showed that the 1 WLM (working level month) concentration of the radon progeny can lead to the annual lung dose of 20  $\text{rads}/\text{year}$ . As recommended by ICRP-30 [35], the annual equivalent dose to the whole lung through the inhalation of the 1  $\text{Bq}/\text{m}^3$  concentration of radon gas should be considered to  $7 \times 10^{-3}$   $\text{mSv}/\text{year}$ .

## Conclusion

The received dose by the lung tissue through the inhalation of the radon gas and exposure to its short-lived daughter radionuclides were evaluated in current study using Monte Carlo simulation. The results showed that the absorbed dose by the lung tissue due to the alpha exposure is quiet higher than the received dose by the beta and gamma decaying products.

Furthermore, the overall received dose by the lung tissue was higher when the radon decay products were deposited within the lung, such that the absorbed dose by the lung in this state was about 100 times higher than the lung dose in the case that the radon progeny were suspended inside the respiratory system.

Finally, it can be concluded that the daughter radionuclides of radon decay are the main concern in terms of internal exposure and corresponding biologic side effects. These radioactive daughter nuclides can be more dangerous than the radon itself. The higher half-life of radon gas makes it possible to escape this radioactive gas from the respiratory system during the exhalation process, while the daughter nuclides are short-lived solid particles which can stick to the inner

wall of the respiratory system and expose the lung tissue for a long period of time.

## References

- Pinti LD, Retaillieu S, Barnetche D, Moreira F, Moritz MA, Larocque M, et al. <sup>222</sup>Rn activity in groundwater of the St. Lawrence Lowlands, Quebec, eastern Canada: relation with local geology and health hazard. *J Environ Radioact.* 2014; 136: 206-17.
- Tsapalov A, Kovler K. Revisiting the concept for evaluation of radon protective properties of building insulation materials. *Building Environ.* 2016; 95: 182-8.
- Bala P, Mehra R, Ramola RC. Distribution of natural radioactivity in soil samples and radiological hazards in building material of Una. Himachal Pradesh. *J Geochem Explor.* 2014; 142: 11-5.
- Moreno V, Bach J, Font L, Baixeras C, Zarroca M, Linares R, et al. Soil radon dynamics in the Amer fault zone: An example of very high seasonal variation. *J Environ Radioact.* 2016; 151: 293-303.
- Giri A, Pant D. Inhalation dose due to Rn-222, Rn-220 and their progeny in indoor environments. *Appl Radiat Isot.* 2018; 132: 116-21.
- Hatif KH, Muttaleb MK, Abbas AH. Measurement of radioactive radon gas concentration of water in the school for kifel. *WSN.* 2016; 54: 191-201.
- Xie D, Liao M, Kearfott KJ. Influence of environmental factors on indoor radon concentration levels in the basement and ground floor of a building- A case study. *Radiat Meas.* 2015; 82: 52-8.
- US Environmental Protection Agency. 2018. Available from: <http://www.epa.gov>.
- Dieguez-Elizondo PM, Gil-Lopez T, O'Donohoe PG, Castejon-Navas J, Galvez-Huerta MA. An analysis of the radioactive contamination due to radon in a granite processing plant and its decontamination ventilation *J Environ Radioact.* 2017; 167: 26-35.
- Papastefanou C. Escaping radioactivity from coal-fired power plants (CPPS) due to coal burning and the associated hazards: A review. *J Environ Radioact.* 2010; 101: 191-200.
- Nevinsky I, Tsvetkova T, Nevinskaya E. Measurement of radon in ground waters of the Western Caucasus for seismological application. *J Environ Radioact.* 2015; 149: 19-35.
- Abojassim AA. Natural radioactivity and radon concentrations in parenteral nutrition samples utilized in Iraqi hospitals. *Iran J Med Phys.* 2019; 16: 1-7.
- Hassanvand H, Hassanvand MS, Birjandi M, Kamarehie B, Jafari A. Indoor radon measurement in dwellings of Khorramabad city, Iran. *Iran J Med Phys.* 2018; 15: 19-27.
- Bu-Olayan AH, Thomas BV. Evaluation of radon pollution in underground parking lots by discomfort index. *Iran J Med Phys.* 2016; 13: 65-76.
- Allahverdi Pourfallah T, Mousavi SM, Shahidi M. Assessment of effective dose equivalent from internal exposure to <sup>222</sup>Rn in Ramsar city. *Iran J Med Phys.* 2015; 12: 36-42.
- Anjos RM, Umisedo N, Da Silva AA, Estellita L, Rizzotto M, Yoshimura EM, et al. Occupational exposure to radon and natural gamma radiation in the La Carolina, a former gold mine in San Luis Province, Argentina. *J Environ Radioact.* 2010; 101: 153-8.
- Rafique M, Rahman S, Rahman SU. Indoor radon concentration measurement in the dwellings of district Poonch (Azad Kashmir), Pakistan. *Radiat Prot Dosimetry.* 2010; 138: 158-65.
- Mostafa AMA, Yamazawa H, Uosif AMA, Moriizumi J. Seasonal behavior of radon decay products in indoor air and resulting radiation dose to human respiratory tract. *J Radiat Res Appl Sci.* 2015; 8: 142-7.
- Ramsiya M, Joseph A, Jojo PJ. Estimation of indoor radon and thoron in dwellings of Palakkad, Kerala, India using solid state nuclear track detectors. *J Radiat Res Appl Sci.* 2017; 10: 269-72.
- Pelowitz DB. MCNPX-A general Monte Carlo N-particle transport code, Version 2.6.0, LA-CP-07-1473. 2008.
- Ochs M, Nyengaard JR, Jung A, Knudsen L, Voigt M, Wahlers T. The number of Alveoli in the human lung. *Am J Respir Crit Care Med.* 2004; 169: 120-4.
- Stone KC, Mercer RR, Freeman BA, Chang LY, Crapo JD. Distribution of lung numbers and volume between alveolar and nonalveolar tissue. *Am Rev Respir Dis.* 1992; 146: 454-6.
- Mostafa MY, Vasyanovich M, Zhukovsky M. A primary standard source of radon-222 based on the HPGe detector. *Appl Radiat Isot.* 2017; 120: 101-5.
- Kim H, Jung Y, Ji YY, Lim JM, Chung KH, Kang MJ. Validation of procedure for the analysis of <sup>226</sup>Ra in naturally occurring radioactive materials using a liquid scintillation counter. *J Environ Radioact.* 2017; 166: 188-94.
- Ishizuka M, Mikami M, Tanaka TY, Igarashi Y, Kita K, Yamada Y, et al. Use of a size-resolved 1-D resuspension scheme to evaluate resuspended radioactive material associated with mineral dust particles from the ground surface. *J Environ Radioact.* 2017; 166: 436-48.
- Lebecki K, Malachowski M, Soltysiak T. Continuous dust monitoring in headings in underground coal mines. *J Sust Min.* 2016; 15: 125-32.
- Battata JBR, Brack J, Daw E, Dorofeev A, Ezeribe AC, Fox JR, et al. Radon in the DRIFT-II directional dark matter TPC: emanation, detection and mitigation. *J Inst.* 2014; 9: P11004.
- Eckerman KF, Endo A. MIRD: Radionuclide data and decay schemes. Second ed. Smmi, the society of nuclear medicine, Reston, VA; 1989.
- Warliah L, Rohman AS, Rusmin PH. Model development of air volume and breathing frequency in human respiratory system simulation. *Procedia Soc Behav Sci.* 2012; 67: 260-8.
- ICRP. The 2007 Recommendations of the International Commission on Radiological Protection. ICRP Publication 103. Ann ICRP. 2007.
- Kendall GM, Smith TJ. Doses to organs and tissues from radon and its decay products. *J Radiol Prot.* 2002; 22: 389-406.
- Smith H. Human respiratory tract model for radiological protection. ICRP publication 66. 1994.
- Yu KN, Lau BM, Nikezic D. Assessment of environmental radon hazard using human respiratory tract models. *J Hazard Mater.* 2006; 132: 98-110.

34. Altshuler B, Nelson N, Kuschner M. Estimation of lung tissue dose from the inhalation of radon and daughters. *Health Phys.* 1964; 10: 1137-61.
35. Vennart J. Limits for intakes of radionuclides by workers: ICRP publication 30. *Health physics.* 1981; 40: 477-84.